Epitrochoids and Hypotrochoids Together Again

Greg Dresden

Greg Dresden (dresdeng@wlu.edu) is a professor of mathematics at Washington & Lee University in the mountains of Virginia. He received his PhD from the University of Texas a great many years ago. He was a living kidney donor in 2018 and he encourages everyone to learn more about this gift of life.

The idea for this article came from a recent problem [**1**] in the *College Mathematics Journal* which asked for the area of one of the four inner loops in Figure 1.

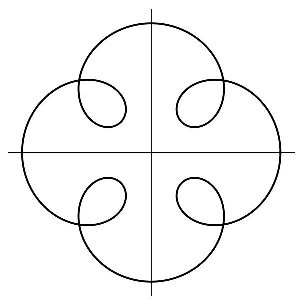

Figure 1. An epitrochoid with four-fold symmetry.

This particular figure is called an *epitrochoid* [**3, 4**] and according to Lawrence [**4**] it dates back to Alfred Dürer's work in 1525. It is described by the parametric equations

$$\begin{aligned} x(t) &= 2\cos t + \cos 5t, \\ y(t) &= 2\sin t + \sin 5t. \end{aligned} \tag{1}$$

An obvious question is why Figure 1 has four-fold symmetry despite the presence of the terms $\cos 5t$ and $\sin 5t$ in equations (1). To answer this question, we can re-write the above pair of equations as a single complex-valued equation. If we let $x(t)$ and $y(t)$ be the real and imaginary part, respectively, of $z(t)$, and if we make use of Euler's identity $e^{it} = \cos t + i \sin t$, then equations (1) become

$$z(t) = x(t) + iy(t) = 2e^{it} + e^{5it} = e^{it}\left(2 + e^{4it}\right), \tag{2}$$

and now the four-fold symmetry is revealed. To be precise, we note that since equation (2) tells us that $z(t) = e^{it}(2 + e^{4it})$, then

$$z(t + \pi/2) = e^{i\pi/2} z(t),$$

which tells us that $z(t + \pi/2)$ has the same modulus as $z(t)$ and is rotated 90° counterclockwise on the complex plane. See Farris [**2**, Ch. 3] and Mutalik [**5**] for more examples of this kind of symmetry argument.

We can see that moving to *complex* variables actually *simplifies* the situation (if you'll forgive the atrocious pun). This does lead to another question: what other discoveries can we make by writing parametric curves in terms of complex variables?

An imperfect nesting To generate a second curve, we decide to make the simplest possible change to equation (2): we replace the e^{4it} with e^{-4it}, giving us the new equation

$$z(t) = e^{it}\left(2 + e^{-4it}\right). \tag{3}$$

When we convert back to Cartesian coordinates, we get a new set of equations,

$$\begin{aligned} x(t) &= 2\cos t + \cos 3t, \\ y(t) &= 2\sin t - \sin 3t, \end{aligned} \tag{4}$$

and this now describes a figure called a *hypotrochoid* [**3, 4**]. Figure 2 shows the dashed hypotrochoid from equations (4), nested inside the solid epitrochoid from equations (1).

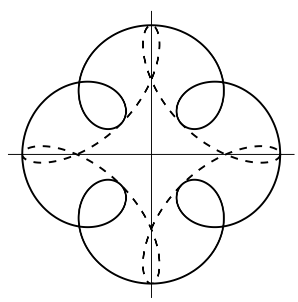

Figure 2. A not-quite-perfect nesting of a solid epitrochoid and dashed hypotrochoid.

From looking at the complex-variable equations $e^{it}\left(2 + e^{4it}\right)$ for the earlier epitrochoid and $e^{it}\left(2 + e^{-4it}\right)$ for the current hypotrochoid, we can see that not only do both have four-fold symmetry but also they clearly intersect each other when the parameter t is a multiple of $\pi/4$, thanks to the convenient fact that $e^{i\pi} = e^{-i\pi}$. Coincidentally, these intersections occur when the polar angle θ is a multiple of $\pi/4$, and this explains why the two curves are nested together as seen in Figure 2. These intersections are also at the maximal modulus and minimal modulus (3 and 1, respectively) for the two complex-variable equations. As we will show later, we can even improve this nesting by slightly altering the graphs.

Epitrochoids and hypotrochoids are often *discussed* together, as they are both formed by tracing the path of a point attached to the radius of one circle that is rolling around the outside (for an epitrochoid) or inside (for a hypotrochoid) of another circle. However, we have not seen them actually *drawn* together as in Figure 2 above and Figures 4 and 6 below. Thanks to our decision to work with complex variables, it was the similarities between equations (2) and (3) that led to our decision to draw them together (as in Figure 2 above) and subsequently led to the other discoveries in this article.

But first, a warning about a common pitfall when talking about complex-variable parametric equations.

The parameter is not always polar It might be tempting to think of the parameter t as measuring the polar angle θ of the point $(x(t), y(t))$ on the Cartesian plane. While the epitrochoid and hypotrochoid from Figure 2 do indeed intersect each other at the polar angle $\theta = 0$ when $t = 0$ (and likewise at θ and t equal to multiples of $\pi/4$ as mentioned above), this is not the case in general. In fact, as the parameter t increases slightly from $t = 0$, the polar angle θ for the point on the hypotrochoid actually *decreases* from $\theta = 0$ before then increasing. We can see this by tracing out the path of the point $(x(t), y(t))$ for the hypotrochoid given by equations (4) as t increases from $t = 0$ in multiples of $\pi/12$, as shown in Figure 3. The origin (not shown) is located to the left of this graph. Note that at $t = \pi/12$ the polar angle θ is slightly negative, and at $t = 2\pi/12$ we have $\theta = 0$. Clearly, t and θ are not always the same.

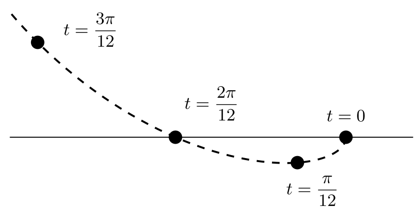

Figure 3. Path of hypotrochoid for small values of t.

A perfect nesting If we move from four-fold to six-fold symmetry by using the equations $z(t) = e^{it}\,(2 + e^{6it})$ and $z(t) = e^{it}\,(2 + e^{-6it})$, we might be surprised at how well the two graphs fit together.

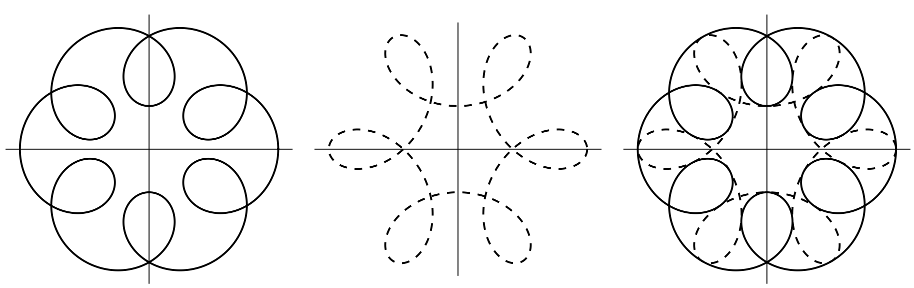

Figure 4. Best possible nesting.

On the left of Figure 4 we have the (solid) epitrochoid with six-fold symmetry, and in the middle is the corresponding six-fold (dashed) hypotrochoid. On the right we can see how they fit together perfectly. The two curves in Figure 4 intersect and are tangent at six “inside” and six “outside” points (just like how the two curves in Figure 2 intersect at four “inside” and four “outside” points). However, these two curves in Figure 4 also intersect and are tangent at twelve “middle” points. See Figure 7 for clarity on what we mean by “inside”, “middle”, and “outside” points.

In Figure 5 we have drawn all twenty-four intersection points for the two curves in Figure 4; the six outside and six inside points of intersection are drawn as solid black dots, and the twelve middle points are drawn as hollow dots. Furthermore, all the six inside points are on a circle of radius 1, the twelve middle points on a circle of radius $\sqrt{3}$, and the six outer points at radius 3; we have drawn these circles as dotted curves.

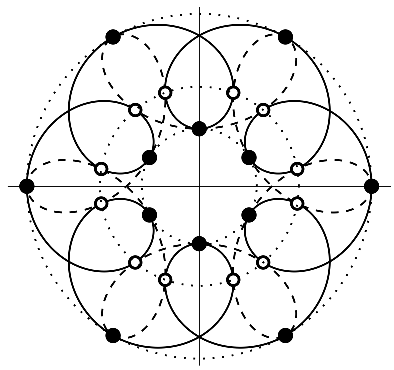

Figure 5. All 24 points of intersection from Figure 4 live on just three circles

As we will now show, we can also achieve this kind of perfect nesting for the four-fold symmetric figures, and in fact for k-fold symmetry for all values of $k > 2$. All we have to do is modify our equations just a little bit.

A more perfect nesting

For context, we show in Figure 6 the best possible nestings for the four, six, and thirteen-fold symmetric epitrochoids and hypotrochoids. The epitrochoids are drawn with solid curves, and the hypotrochoids with dashed curves. The scale is the same in all three.

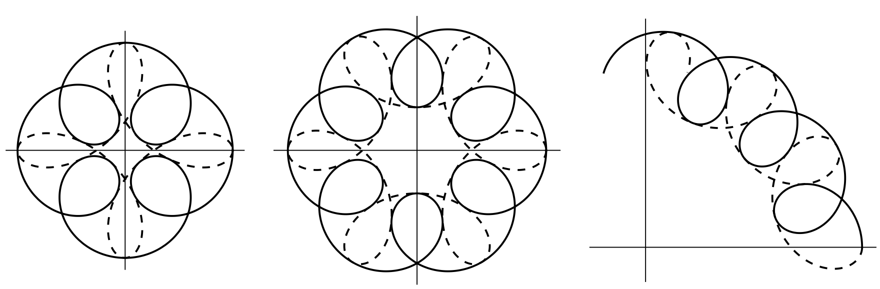

Figure 6. More perfect nestings for $k = 4, 6$, and 13.

We say this is a *perfect nesting* when the epitrochoid and hypotrochoid of k-fold symmetry are tangent at k points of intersection on the inside, $2k$ points of intersection in the middle, and k points of intersection on the outside. See Figure 7.

We mentioned earlier that we can achieve perfect nesting if we "... modify our equations just a little bit". As the following theorem shows, we simply need to modify the "2" in equations (1) and (4) to a new value that is dependent on k.

Theorem 1 (Nesting Theorem). *For the epitrochoid (x_e, y_e) and hypotrochoid (x_h, y_h) of k-fold symmetry defined as*

$$(x_e, y_e) = (A_k \cos t + \cos(k+1)t, A_k \sin t + \sin(k+1)t),$$
$$(x_h, y_h) = (A_k \cos t + \cos(k-1)t, A_k \sin t - \sin(k-1)t)$$

with $k > 2$, we have perfect nesting when $A_k = \csc(\pi/k)$. Furthermore, the inside and outside points of intersection are on circles of radii $\csc(\pi/k) - 1$ and $\csc(\pi/k) + 1$ respectively, and the middle points are on a circle of radius $\cot(\pi/k)$.

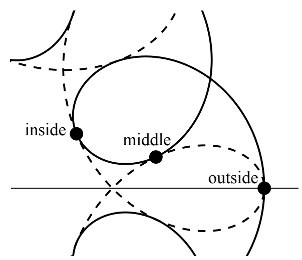

Figure 7. Points of intersection and tangency.

As an example, we note that for $k = 6$ this theorem tells us that $A_6 = \csc(\pi/6) = 2$, which gives us the perfect nesting in Figure 4, and it tells us that the radii of the circles for the intersection points are $\csc(\pi/6) - 1, \csc(\pi/6) + 1$, and $\cot(\pi/6)$ which give us the circles of radii $1, 3$, and $\sqrt{3}$ as seen in Figure 5. Our epitrochoid and hypotrochoid equations in this case would be

$$(x_e, y_e) = (2\cos t + \cos 7t, 2\sin t + \sin 7t),$$
$$(x_h, y_h) = (2\cos t + \cos 5t, 2\sin t - \sin 5t).$$

Likewise, for $k = 4$ the epitrochoid and hypotrochoid in equations (1) and (4) as seen in Figure 2 do not have perfect nesting. To achieve the perfect nesting, we would simply need to replace the 2 in equations (1) and (4) with $A_4 = \csc(\pi/4) = \sqrt{2}$; the result is seen in the picture on the left of Figure 6. The corresponding equations for the epitrochoid and hypotrochoid would be

$$(x_e, y_e) = (\sqrt{2}\cos t + \cos 5t, \sqrt{2}\sin t + \sin 5t),$$
$$(x_h, y_h) = (\sqrt{2}\cos t + \cos 3t, \sqrt{2}\sin t - \sin 3t).$$

The reader should compare these to the not-quite-perfect equations (1) and (4).

Proof of Theorem 1. As mentioned earlier, there are inherent advantages in writing our Cartesian equations in terms of complex variables. Starting with the equations for the epitrochoid in the statement of Theorem 1, we define $z_e(t)$ as $x_e(t) + iy_e(t)$. This gives us

$$z_e(t) = A_k(\cos t + i\sin t) + (\cos(k+1)t + i\sin(k+1)t),$$

and when we apply Euler's identity and simplify, we get

$$z_e(t) = A_k e^{it} + e^{i(k+1)t} = e^{it}\left(A_k + e^{ikt}\right). \tag{5}$$

Likewise, with the equations for the hypotrochoid in the statement of Theorem 1, we define $z_h(t)$ as $x_h(t) + iy_h(t)$. This gives us

$$z_h(t) = A_k(\cos t + i\sin t) + (\cos(k-1)t - i\sin(k-1)t),$$

and when we again apply Euler's identity and then simplify, we get

$$z_h(t) = A_k e^{it} + e^{-i(k-1)t} = e^{it}\left(A_k + e^{-ikt}\right). \tag{6}$$

We can now clearly see that both curves have k-fold rotational symmetry since

$$z_e(t + 2\pi/k) = e^{i2\pi/k} z_e(t) \qquad \text{and} \qquad z_h(t + 2\pi/k) = e^{i2\pi/k} z_h(t),$$

telling us that when we increase t by $2\pi/k$ we get a point with the same modulus but rotated $2\pi/k$ counterclockwise.

At this point, we could simply study a sector of angular width $2\pi/k$ and then appeal to the k-fold symmetry. However, we can do a bit more. Since

$$z_e(-t) = \overline{z_e(t)} \qquad \text{and} \qquad z_h(-t) = \overline{z_h(t)},$$

both graphs are symmetric across the x-axis as well. This means that we need only focus our attention on the sector in the first quadrant from the horizontal axis to the ray at polar angle $\theta = \pi/k$ measured counterclockwise from the horizontal. See Figure 8 for an illustration.

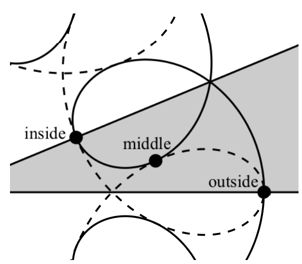

Figure 8. By symmetry, we need only consider this one sector from $\theta = 0$ to $\theta = \pi/k$.

With this in mind, we start by showing that the two curves do indeed intersect at the outside and inside points by noting that

$$z_e(0) = A_k + 1 = z_h(0)$$

and

$$z_e(\pi/k) = e^{i\pi/k}(A_k - 1) = z_h(\pi/k).$$

The moduli of these complex numbers above are $A_k + 1$ and $A_k - 1$, giving us the radii of the circles for the outside and inside points of intersection as mentioned in the theorem. Since these are the maximum and minimum values, respectively, for the moduli of the two curves, we know that both curves are in fact tangent to the circle of radius $A_k + 1$ (on the outside) or $A_k - 1$ (on the inside) at those points of intersection and hence are tangent to each other.

We now turn our attention to the middle points of intersection, as seen in Figure 8. Here, things are a little bit more difficult because the epitrochoid and hypotrochoid actually "intersect" at that middle point at different values of the parameter t. To be precise, we set $\phi = \pi/2k - \pi/k^2$ and we will show that

$$z_e(\phi + \pi/k) = z_h(\phi - \pi/k) \tag{7}$$

and that their moduli is $\cot(\pi/k)$. We can then appeal to symmetry to cover the other $2k - 1$ middle points. (We should note that we only arrived at equation (7) after a considerable amount of guess-and-check.)

For the left-hand side of equation (7), we use the expression for z_e in equation (5), replacing A_k with $\csc(\pi/k)$ and replacing t with $\phi + \pi/k$, to get

$$\begin{aligned} z_e(\phi + \pi/k) &= e^{i\phi} e^{i\pi/k} \left(\csc(\pi/k) + e^{i\pi/2} e^{-i\pi/k} e^{i\pi} \right) \\ &= e^{i\phi} \left(e^{i\pi/k} \csc(\pi/k) + e^{i\pi/2} e^{i\pi} \right) \\ &= e^{i\phi} \left(\frac{\cos(\pi/k) + i \sin(\pi/k)}{\sin(\pi/k)} - i \right) = e^{i\phi} \cot(\pi/k). \end{aligned}$$

Likewise, for the right-hand side of equation (7), we use the expression for z_h in equation (6) but this time replacing t with $\phi - \pi/k$, to get

$$\begin{aligned} z_h(\phi - \pi/k) &= e^{i\phi} e^{-i\pi/k} \left(\csc(\pi/k) + e^{-i\pi/2} e^{i\pi/k} e^{i\pi} \right) \\ &= e^{i\phi} \left(e^{-i\pi/k} \csc(\pi/k) + e^{-i\pi/2} e^{i\pi} \right) \\ &= e^{i\phi} \left(\frac{\cos(\pi/k) - i \sin(\pi/k)}{\sin(\pi/k)} + i \right) = e^{i\phi} \cot(\pi/k). \end{aligned}$$

This verifies equation (7), as desired. Note that we have also verified that the modulus in each case is $\cot(\pi/k)$, giving us the desired radius for the circle containing these middle points of intersection.

It remains to show that the two curves are tangent at that point of equality in equation (7). For this, we recall that the slope of the tangent line to a parametric curve $(x(t), y(t))$ is given by $(dy/dt)/(dx/dt)$. Once more we rely on complex variables to simplify the problem, thanks to the nice property that if $z(t) = x(t) + iy(t)$ then $dx/dt = \text{Re}\, z'(t)$ and $dy/dt = \text{Im}\, z'(t)$, for the real and imaginary parts respectively. Thus, referring back to equation (7), if we can also show that

$$z_e'(\phi + \pi/k) = z_h'(\phi - \pi/k), \tag{8}$$

this would imply the real and the imaginary parts of equation (8) are the same, and so the slopes of the tangent lines would be the same at that point of intersection.

For the left-hand side of equation (8), we write $z_e(t) = A_k e^{it} + e^{i(1+k)t}$, so that

$$z_e'(t) = iA_k e^{it} + i(1 + k)e^{i(1+k)t}$$

$$= ie^{it}\left(A_k + (1+k)e^{ikt}\right). \tag{9}$$

Now, for $t = \phi + \pi/k$ as seen on the left of equation (8), and with $\phi = \pi/2k - \pi/k^2$ as before, we note that

$$kt = (\pi/2 - \pi/k) + \pi$$

and so

$$e^{ikt} = e^{i\pi/2}e^{-i\pi/k}e^{i\pi} = -ie^{-i\pi/k}.$$

This means that equation (9) becomes

$$\begin{aligned} z_e'(\phi + \pi/k) &= ie^{i\phi}e^{i\pi/k}\left(A_k - i(1+k)e^{-i\pi/k}\right) \\ &= ie^{i\phi}\left(A_k e^{i\pi/k} - i(1+k)\right). \end{aligned} \tag{10}$$

Keeping that aside for now, we next turn to the right-hand side of equation (8). We write $z_h(t) = A_k e^{it} + e^{i(1-k)t}$, which means that

$$\begin{aligned} z_h'(t) &= iA_k e^{it} + i(1-k)e^{i(1-k)t} \\ &= ie^{it}\left(A_k + (1-k)e^{-ikt}\right). \end{aligned} \tag{11}$$

Now, for $t = \phi - \pi/k$ as seen on the right of equation (8), and with $\phi = \pi/2k - \pi/k^2$ as before, we note that this time,

$$kt = (\pi/2 - \pi/k) - \pi$$

and so

$$e^{-ikt} = e^{-i\pi/2}e^{i\pi/k}e^{i\pi} = ie^{i\pi/k}.$$

This means that equation (11) becomes

$$\begin{aligned} z_h'(\phi - \pi/k) &= ie^{i\phi}e^{-i\pi/k}\left(A_k + i(1-k)e^{i\pi/k}\right) \\ &= ie^{i\phi}\left(A_k e^{-i\pi/k} + i(1-k)\right). \end{aligned} \tag{12}$$

We now compare equations (10) and (12) to show that they are indeed equal to each other. We start with the expression inside the parentheses in (10), which is

$$\left(A_k e^{i\pi/k} - i(1+k)\right) = \frac{\cos(\pi/k) + i\sin(\pi/k)}{\sin(\pi/k)} - i(1+k) = \cot(\pi/k) - ik. \tag{13}$$

Likewise, the expression inside the parentheses in equation (12) is

$$\left(A_k e^{-i\pi/k} + i(1-k)\right) = \frac{\cos(\pi/k) - i\sin(\pi/k)}{\sin(\pi/k)} + i(1-k) = \cot(\pi/k) - ik. \tag{14}$$

Since these are the same, then equations (10) and (12) are equal to each other, which establishes the equality in (8), thus showing that the two curves are indeed tangent, as desired. ■

A surprising slope

The highlight in the proof of Theorem 1 was showing that the epitrochoid and hypotrochoid are indeed tangent at the middle point of intersection as seen in Figure 7. This slope exhibits a rather unusual behavior as we increase the value of k, as shown in Figure 9. Despite the large value of k for the graphs on the right of Figure 9, the teardrop

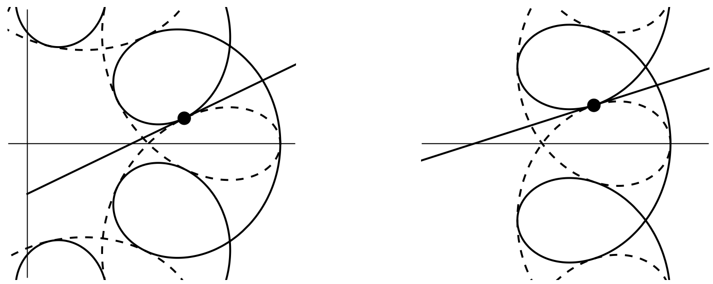

Figure 9. Tangent line at first middle point of intersection for $k = 7$ and $k = 2000$.

shapes for the (solid) epitrochoid and the (dashed) hypotrochoid remain slightly askew, which means the tangent line at that middle point of intersection is not horizontal, nor will it approach horizontal even as k continues to increase. In fact, the limiting value for the slope of this tangent line is rather surprising.

Theorem 2 (Slope Theorem). *For the epitrochoid and hypotrochoid in Theorem 1 with perfect nesting at $A_k = \csc(\pi/k)$, the slope of the tangent line at the first middle point of intersection above the x-axis approaches $1/\pi$ as $k \to \infty$.*

Proof. Recall from our discussion in the proof of Theorem 1 that the slope of the tangent line is equal to $(dy/dt)/(dx/dt)$ which is equal to $\operatorname{Im} z'(t)/\operatorname{Re} z'(t)$. We look now to equation (10) which gives us the derivative z' of the epitrochoid (and the hypotrochoid as well) at the point of intersection as

$$z' = ie^{i\phi}\left(A_k e^{i\pi/k} - i(1+k)\right),$$

where $\phi = \pi/2k - \pi/k^2$. Thanks to equation (13) this becomes

$$z' = ie^{i\phi}\left(\cot(\pi/k) - ik\right) = i\left(\cos\phi + i\sin\phi\right)\left(\cot(\pi/k) - ik\right),$$

and if we multiply this out and simplify, we obtain

$$z' = \left(k\cos\phi - \cot(\pi/k)\sin\phi\right) + i\left(k\sin\phi + \cot(\pi/k)\cos\phi\right).$$

Since the slope is $m = \operatorname{Im} z'/\operatorname{Re} z'$, we get

$$m = \frac{k\sin\phi + \cot(\pi/k)\cos\phi}{k\cos\phi - \cot(\pi/k)\sin\phi}.$$

We multiply top and bottom by $\sin(\pi/k)$ to obtain

$$m = \frac{k\sin(\pi/k)\sin\phi + \cos(\pi/k)\cos\phi}{k\sin(\pi/k)\cos\phi - \cos(\pi/k)\sin\phi}.$$

We can now take the limit as $k \to \infty$. Recall that $\phi = \pi/2k - \pi/k^2$, so as $k \to \infty$ then $\phi \to 0$. A simple application of L'Hôpital's rule tells us that $k \sin(\pi/k)$ approaches π as $k \to \infty$, and so

$$m \to \frac{\pi \sin 0 + \cos 0 \cos 0}{\pi \cos 0 - \cos 0 \sin 0} = \frac{1}{\pi},$$

as desired. ∎

A few more limiting values

As we saw in Theorem 2, our epitrochoid and hypotrochoid have interesting geometries in the limit as k goes to infinity. We encourage the reader to try their hand at the following problems (as suggested by our helpful anonymous referee).

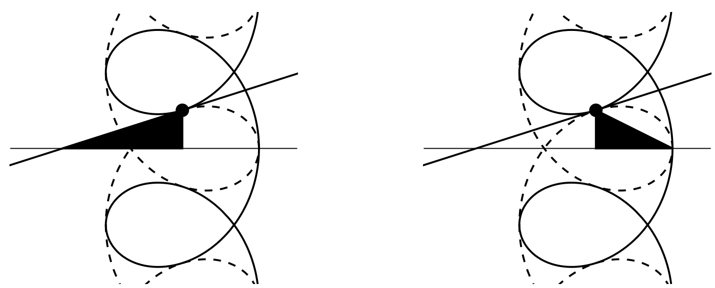

Figure 10. Two triangles related to the tangent line.

In Figure 10, the black line is the same tangent line as referenced in Theorem 2.

1. Show that the area of the black triangle on the left of Figure 10 approaches $\pi/8$ as $k \to \infty$.
2. Likewise, show that the area of the black triangle on the right approaches $1/4$.

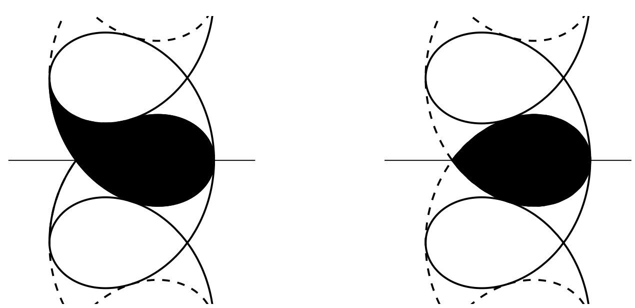

Figure 11. Two areas related to the hypotrochoid.

In Figure 11, we have shaded in two regions related to the hypotrochoid.

1. Show that the area of the black paisley shape on the left of Figure 11 approaches $\pi/2$ as $k \to \infty$.
2. We do not have a simple expression for the area of the teardrop shape on the right of Figure 11. We encourage the reader to give it a try.

Conclusion

As we have seen, the epitrochoid and hypotrochoid reveal some surprising secrets when written in complex variables. We can only wonder what other parametric curves might benefit from a similar treatment.

Summary. Two classic plane curves, the epitrochoid and hypotrochoid, can be placed together in an optimal nested form. We find the appropriate equations by way of complex variables, and we also get a surprising answer for the slope of a particular tangent line.

References

1. Dresden, G. (2024). Problem #1274. *Coll. Math. J.* 55(2): 176.
2. Farris, F. A. (2015). *Creating Symmetry. The Artful Mathematics of Wallpaper Patterns*. Princeton, NJ: Princeton University Press.
3. Gray, A., Salamon, S., Abbena, E. (2006). *Modern Differential Geometry of Curves and Surfaces with Mathematica*. Boca Raton, FL: Chapman & Hall/CRC.
4. Lawrence, J. (1972). *A Catalog of Special Plane Curves*. New York, NY: Dover Publications.
5. Mutalik, P. (2015). Solution: 'Creating Art With Mathematics', *Quanta*. Available at `https://www.quantamagazine.org/solution-creating-art-with-mathematics-20151030/`